[21]Nickle, W. E. and Sims, L. W., "Study and Exploratory Free-Flight Investigation of Deployable Aerodynamic Decelerators Operating at High Altitudes and at High Mach Numbers," FDL-TDR-64-35, Vol. I, July 1964, Air Force Flight Dynamics Lab., Wright-Patterson Air Force Base, Ohio.

[22]Turner, R. and McMullen, J. C., "Feasibility of Parachute Operation at High Mach Numbers and Dynamic Pressures," AIAA Paper 66-24, New York, 1966.

[23]Bloetscher, F. and Arnold, W. V., "Aerodynamic Deployable Decelerator Performance-Evaluation Program," AFFDL-TR-67-60, October 1967, Air Force Flight Dynamics Lab., Wright-Patterson Air Force Base, Ohio.

[24]MacLanahan, D. A., "An Investigation of Various Types of Decelerators at Mach Number 2.8," AEDC-TR-66-136, July 1966, Arnold Engineering Development Center, Arnold Air Force Station, Tullahoma, Tenn.

[25]French, K. E., "Model Law for Parachute Opening Shock," *AIAA Journal*, Vol. 2, No. 12, Dec. 1964, pp. 2226–2228.

[26]Fredette, R. O., "Parachute Research Above Critical Aerodynamic Velocities," Rept. P-1031C, 1961, Cook Research Laboratories, Morton-Grove, Ill.

[27]Greene, G. C., "Opening Distance of a Parachute," *Journal of Spacecraft and Rockets*, Vol. 7, No. 1, Jan 1970, pp. 98–100.

[28]Dickie, G. D., "Tests of FIST Ribbon Parachutes in the UAC Subsonic Wind Tunnel," United Aircraft Corporation Rept. R-1408-1, Feb. 1959, East Hartford, Conn.

[29]Ibrahim, S. K., "Potential Flowfield and Added Mass of the Idealized Hemispherical Parachute," *Journal of Aircraft*, Vol. 4, No. 2, March-April 1967, pp. 96–100.

[30]Ibrahim, S. K., "Experimental Determination of the Apparent Moment of Inertia of Parachutes," AFFDL-TDR-64-153, April 1965, Air Force Flight Dynamics Lab., Wright-Patterson Air Force Base, Ohio.

[31]Milne-Thomson, L. M., *Theoretical Hydrodynamics*, 5th edition, MacMillan Co., New York, 1968, p. 479.

[32]Ewing, E. G., "Ringsail Parachute Design," AFFDL-TR-72-3, January 1972, Air Force Flight Dynamics Lab., Wright-Patterson Air Force Base, Ohio.

JANUARY J. AIRCRAFT VOL. 11, NO. 1

A Conceptual Study of Leading-Edge-Vortex Enhancement by Blowing

R. G. Bradley* and W. O. Wray†
General Dynamics, Fort Worth, Texas

A conceptual wind-tunnel-test program has been conducted to verify that blowing a stream of high-pressure air over a swept-wing surface in a direction roughly parallel to the leading edge enhances the vortex system. The blowing is shown to intensify the leading-edge vortex and thus delay the deleterious effects of vortex breakdown to higher angle of attack. As a result, the vortex-lift is significantly increased and, as the blowing rate is increased, appears to approach the value predicted by the Polhamus suction-analogy for thin wings.

Nomenclature

AR = aspect ratio
C = wing root chord
C_w = root chord of theoretical trapezoidal wing
C_D = drag coefficient
C_L = lift coefficient
C_M = moment coefficient about ¼ MAC
C_μ = momentum coefficient
C_{Do} = zero-lift drag coefficient
α = angle-of-attack

Introduction

DESIGN concepts that take advantage of vortex lift play an important part in improving maneuverability of current air-superiority fighters. Further, takeoff and landing performance of other advanced aircraft, e.g., supersonic aircraft, rely to a large extent upon favorable leading-edge vortex-induced effects.

The use of concentrated blowing to enhance and strengthen a wing leading-edge-vortex system, of the type illustrated in Fig. 1, can offer significant improvements in lifting efficiency. The stability of a vortex is known to be related to the longitudinal flow along the axis of the vortex. Ringleb[1] noted the importance of the vortex-core flow in early attempts to establish a stationary vortex for flow control. The application of spanwise blowing to increase lift has been described by Cornish,[2] and spanwise flap blowing has been shown by Dixon[3] to increase the flap-lift increment. In flow visualization studies at ONERA, Werle[4] has shown that leading-edge-vortex breakdown can be controlled on delta wings by concentrated blowing along the vortex axis.

Some of the benefits of vortex enhancement are noted in Fig. 1. For wings with high leading-edge sweep, the augmented natural vortex results in an increased vortex-lift increment. For wings with low leading-edge sweep, the blowing aids in the formation of the leading-edge vortex, thus developing vortex lift where none is developed naturally. Vortex breakdown is delayed to higher angles of at-

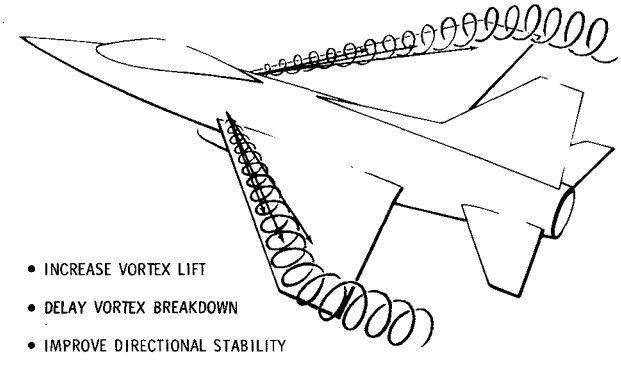

Fig. 1 Blowing concept for vortex enhancement.

Presented as Paper 73-656 at the AIAA 6th Fluid and Plasma Dynamics Conference, Palm Springs, Calif., July 16–18, 1973; submitted July 11, 1973.

Index categories: Aircraft Aerodynamics; Subsonic and Transonic Flow.

*Design Specialist, Aerospace Technology Dept., Convair Aerospace Div. Associate Fellow AIAA.

†Senior Aerodynamics Engineer, Aerospace Technology Dept., Convair Aerospace Div.

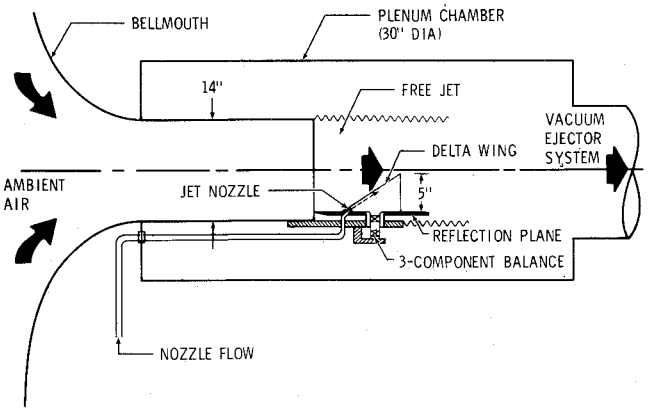

Fig. 2 Force-test wind tunnel schematic.

tack, resulting in improved buffet characteristics. The enhanced wing vortex system is expected to improve directional stability by avoiding the adverse effects of vortex breakdown in the vicinity of the horizontal and vertical tail. Very high blowing rates may provide additional lift benefits by effectively increasing the aspect ratio of the wing.

The conceptual test program reported in this paper was designed to investigate the effects of blowing for swept-wing planforms typical of fighter aircraft. Low-speed tests conducted at the Fort Worth operation of the Convair Aerospace Division produced force and moment data to verify the blowing effectiveness and flow-visualization data to gain understanding of the basic flow mechanism.

Wind Tunnel Tests

Test Facilities

Force testing was accomplished in a freejet wind tunnel. A reflection plane surface, located at the exit of a 14-in.-square test section, was used for mounting the semi-span wings used in the investigation. A schematic of the tunnel is shown in Fig. 2. Ambient air is drawn into a large bell-mouth inlet where it converges into a 14-in.-square test section. The test section exits into a large plenum chamber, which is connected to an ejector system. Pressure orifices located near the test section exit are utilized to determine freestream velocity for the freejet flow.

Flow-visualization studies were performed in a 14-in.-square, closed-test-section smoke tunnel at the Fort Worth facility. A schematic is shown in Fig. 3. The reflection plane and model were mounted as in the freejet installation. The smoke generator apparatus provided an array of smoke filaments to the low-turbulence test section. Glass panels on three sides of the test section permitted visual observation and photography.

Models and Instrumentation

The reflection-plane surface was used to support a five-component moment-type balance for force measurements

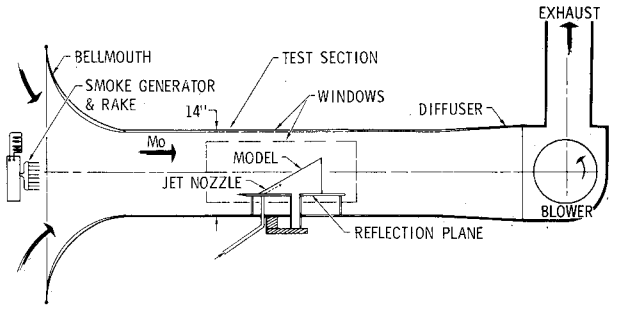

Fig. 3 Smoke tunnel schematic.

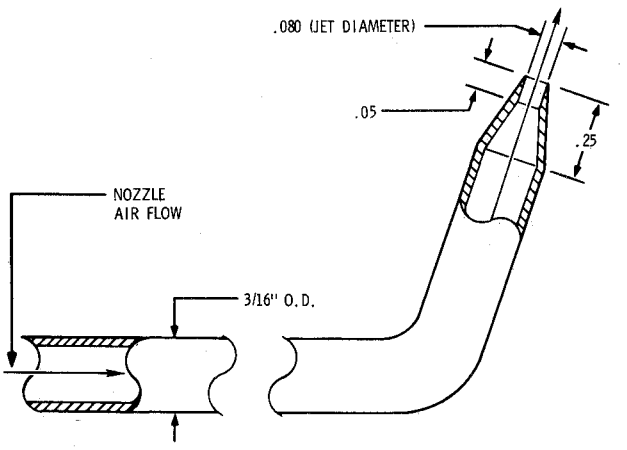

Fig. 4 Convergent nozzle details.

and to position a convergent nozzle for directing air over the model surface. A high-pressure air source supplied the required nozzle flow rates.

A simple convergent nozzle, as shown in Fig. 4, was used in these tests. As each model required a "unique" nozzle angle for flow direction, several flow nozzles were required, each of which was calibrated with a laboratory standard flow metering device.

Three wing planforms, shown in Fig. 5, were tested. The wings were simple flat plates, with all edges beveled to a sharp edge. The span for each was five in. The convergent nozzles were positioned to blow parallel to the leading edge of each wing with several chordwise positions available. The nozzle was attached to the reflection plane and was not in contact with the wing-balance system. Thus the forces measured are purely aerodynamic and do not include nozzle thrust components.

Angles of attack up to 30° were achieved by rotating the model and the reflection plane simultaneously. The rotation procedure maintained a nonvarying nozzle-distance-to-model-surface relationship of approximately one nozzle diameter.

Force Tests

Force and moment data were taken for nominal test conditions of $M_0 = 0.30$ and Reynolds number per foot of 1.8×10^6. Jet blowing was varied up to the maximum total pressure available (215 psia), and a blowing momentum coefficient, defined as $C_\mu = \dot{m}V_j/q_\infty S$, was computed from the measured mass flow rate, $\dot{m}$, and the fully expanded isentropic jet velocity, V_j.

As a result of the combined effects of reflection plane testing and the freejet tunnel, the half-span low-AR wings generated a lift-curve slope that is some 10–20% lower than would be expected for full-span wings in free

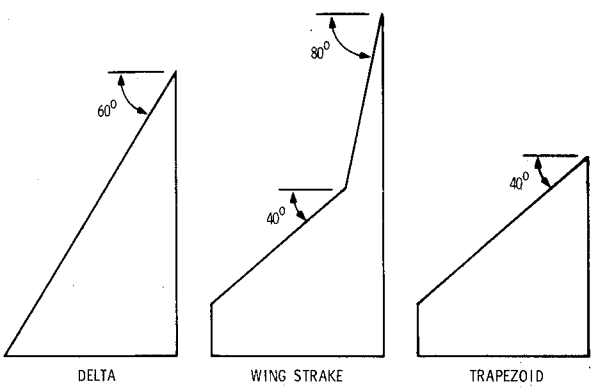

Fig. 5 Wing planforms tested.

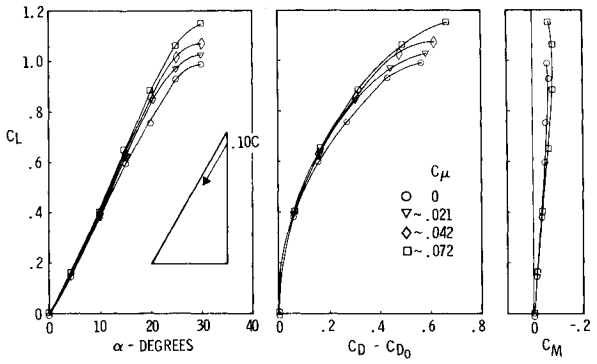

Fig. 6 Delta-wing force data.

air. No corrections to the data were made for either half-span or freejet effects. The objectives of the conceptual tests are not impaired by reduced lift forces of the semi-span wings since the relative leading-edge vortex-enhancement effects due to blowing are clearly evident.

As many as five chordwise locations were available for jet positioning with each model. The test technique involved setting the wing at a 25° angle of attack. Each nozzle position was, in turn, varied from no flow to $C_\mu \sim 0.09$, and force data were taken at several intervals. From these data comparisons, the best nozzle position was determined for each model as the position corresponding to the greatest increase in lift with blowing. A full-pitch polar was then performed at 5° increments up to 30° while varying C_μ at each angle.

Flow Visualization

Studies utilizing a smoke tunnel facility were performed to permit a visual analysis of the vortex-enhancement phenomena. The testing was performed at a nominal free-stream velocity of 50 fps. The wings were painted black for high contrast with the smoke filaments, and angle of attack was set prior to smoke tunnel operations. Full freedom in locating the smoke-filament rake was available to insure filament impingement on the model at the desired locations. At selected conditions, photographs were made of the model/flowfield relationship with and without leading-edge blowing. Force data were not recorded during the flow-visualization test.

Results and Discussion

Some of the pertinent results of the study are presented. In all cases, the nozzle was positioned one exit diameter above the wing, and a brief chordwise position study was performed to locate the most effective blowing location. The data presented below reflect the nozzle positions selected as best for each planform.

Delta-Wing Results

Typical force and moment data for the delta-wing configuration are summarized in Fig. 6. A chordwise location of 0.10C was selected as best for the delta wing. Blowing is noted to result in significant increases in lift, especially at the higher angles of attack. The attendant improvement in drag polar shape at high C_L is apparent.

The vortex-enhancement effect is illustrated by the smoke-streamline photographs shown in Fig. 7. At the 25° angle of attack, the leading-edge vortex without blowing is shed across the midspan of the wing. With blowing, the vortex is seen to be tightened and lie along the wing leading edge. The large value of C_μ achieved in the smoke tests is a result of the low-q test conditions for the flow visualization tests. Even though the smoke photographs

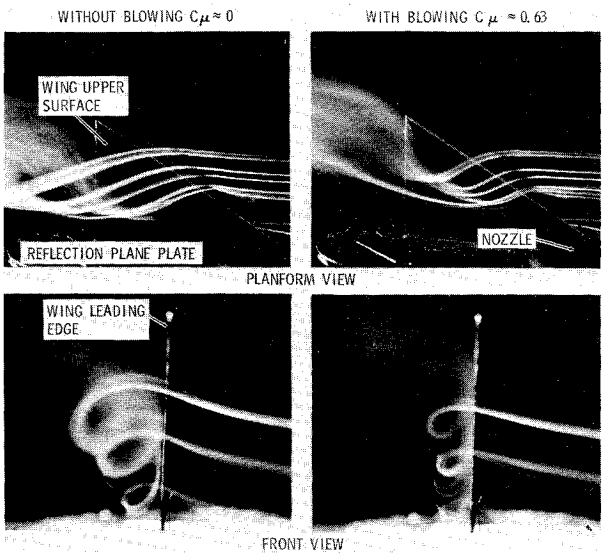

Fig. 7 Delta-wing streamlines, $\alpha = 25°$.

are for C_μ values considerably higher than those for the force measurements, the qualitative effects of blowing are accurately portrayed. It was noted that the flow field instantly changed to a pattern very similar to the one shown as soon as the air supply valve was cracked, even when supply pressures were far below that required to choke the convergent nozzle.

In order that the results could be assessed in the light of other experimental data and theory, the delta-wing data were adjusted to compare with the full-span data of Wentz and Kohlman.[5] A multiplying factor of 1.2 was found to bring the nonblowing lift data into agreement with the data of Ref. 5. The same factor, 1.2, was then applied to the blowing data for $C_\mu \sim 0.07$. The results are compared in Fig. 8, where the leading-edge-suction analogy theory developed by Polhamus[6] is also shown.

The effect of blowing is noted to increase the lift to the full vortex-lift level predicted by theory. The deviation of the nonblowing lift curve from the theory has been attributed by Polhamus to the movement of the vortex breakdown location from the trailing edge to the wing apex with angle of attack. This vortex-breakdown movement for the 60° delta has been measured by Wentz and Kohlman. The beginning and ending of the phenomenon are indicated in Fig. 8. The upper-surface blowing, at least for

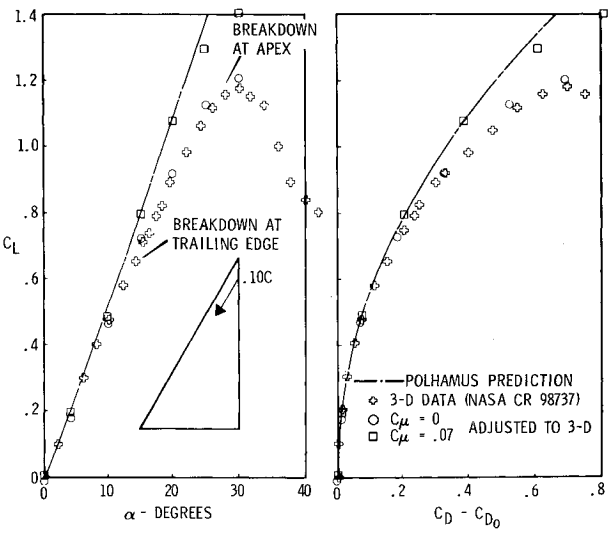

Fig. 8 Comparison with theory—delta wing.

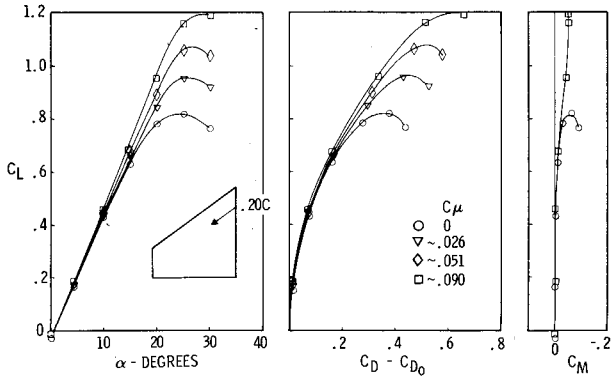

Fig. 9 Trapezoidal-wing force data.

the C_μ range considered here, delays the vortex-breakdown process and thus improves the lift and drag characteristics of the wing.

Trapezoidal-Wing Results

A summary of the force and moment data for the trapezoidal planform is presented in Fig. 9. A chordwise nozzle position of 0.20C was selected. Significant improvements in the lift and drag polar without adverse pitching moment effects are seen to result from blowing at the higher angles of attack. Wentz and Kohlman noted that for their 45° delta wing no observable leading-edge vortex was formed. For the 40°-sweep trapezoidal wing, longitudinal blowing stabilizes and aids in formation of the leading-edge vortical flow.

The effect is clearly illustrated in Fig. 10 by the smoke streamline pictures taken at $\alpha = 25°$. Without blowing, the wing is seen to be completely stalled. When blowing is applied, a strong vortex is noted to lie along the leading edge of the wing upper surface. Increasing C_μ has the effect of strengthening the vortex, as is evidenced in the force data of Fig. 9 and in the series of smoke pictures in Fig. 10. At the high blowing rates shown in Fig. 10, the increased vortex intensity is apparent with the increasing C_μ by the increased entrainment of smoke streamlines lying outboard of the wing tip.

Blowing effectiveness for increasing lift is displayed in Fig. 11 in terms of normalized C_L versus C_μ. The lift

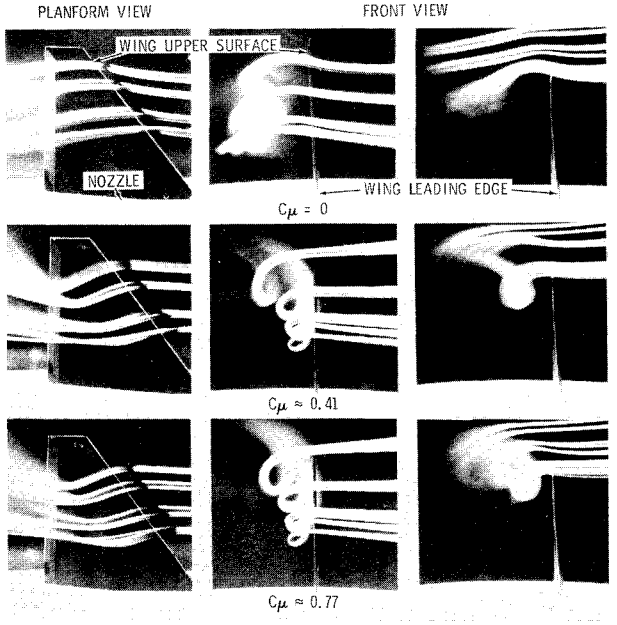

Fig. 10 Trapezoidal-wing streamlines, $\alpha = 25°$.

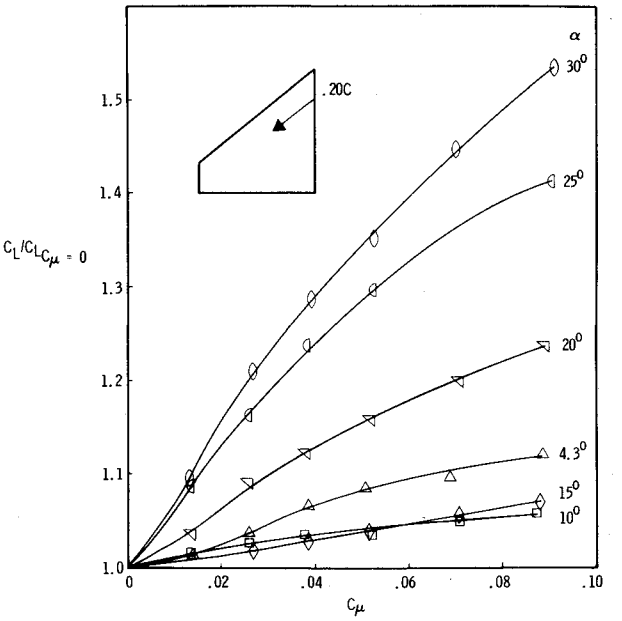

Fig. 11 Blowing effectiveness for the trapezoidal wing.

with blowing is divided by the nonblowing lift value. Lift improvement of up to 50% is noted for the high momentum coefficients at 30° angle of attack.

Wing-Strake Results

The wing-strake configuration was tested by blowing at the strake and, then, at the outer wing panel. In the latter case, the nozzle was positioned both in the reflection plane and extended from the wall to a spanwise location just outboard of the strake-wing intersection point.

Wing-Panel Blowing. The wing-panel blowing data are summarized in Figs. 12 and 13. The extended-nozzle data were taken by simply extending the supply tube through the wall to the wing-strake intersection location. The blowing is seen to be effective for both nozzle locations, with the extended nozzle proving to be slightly better. A nozzle-position study was made only for the case with

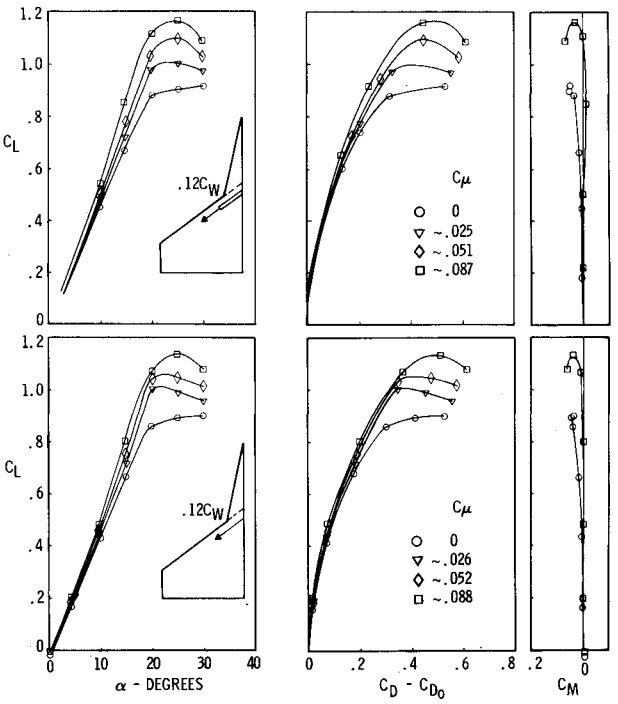

Fig. 12 Wing-strake force data—panel blowing.

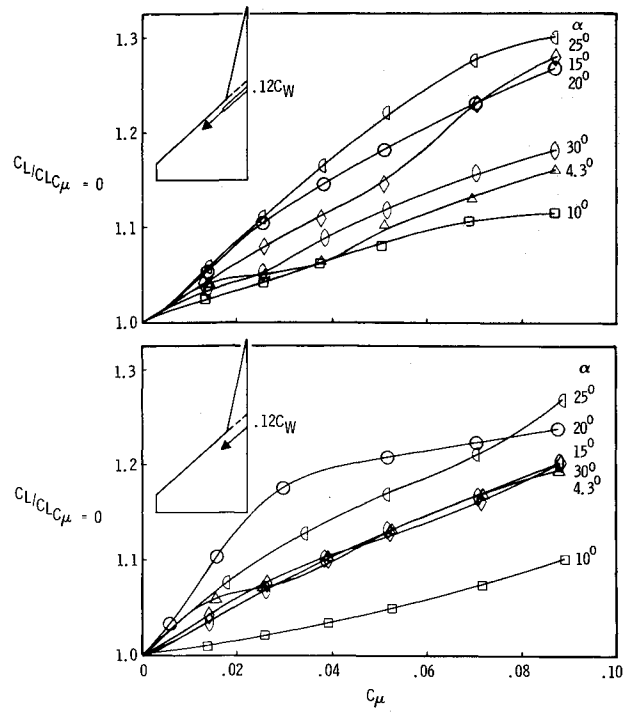

Fig. 13 Blowing effectiveness for the wing-strake planform.

blowing from the wall. Unlike the delta and trapezoidal wings, the blowing effectiveness was found to be relatively insensitive to position in the range 0 to 0.20 of the wing-panel root chord C_w. A position of 0.12 C_w was selected.

The flow phenomena for the wing-strake planform are influenced by the strake-vortex system. With no blowing, the strake vortex is generated at low angles of attack and, as alpha is increased, the vortex turns outboard into the stalled outer-panel flow, where breakdown occurs with further increase in angle of attack. The position of the strake vortex in the plane perpendicular to the wing trailing edge is shown in Fig. 14 for two angles of attack. The visual technique involved passing a smoke streamline over the strake and illuminating the plane at the wing trailing edge with a laser source. The film was exposed twice: first to record the vortex smoke in the plane of the trailing edge and, then, with lights on, to illuminate the model and smoke filament. The movement of the vortex-flow outboard and the diffusion of the smoke associated with the breakdown phenomena is apparent at $\alpha = 20°$.

The flow pattern at 20° angle of attack with and without blowing is shown in Fig. 15. The outboard drift of the strake vortex with no blowing is evident. Blowing completes the turning of the strake vortex so that a single vortex is formed, beginning on the strake and following the panel leading edge to the tip, where it is then shed downstream.

Some further details of the vortex system are shown in Fig. 16 for $\alpha = 25°$. Here, without blowing, the strake vortex breaks down immediately after turning outboard and

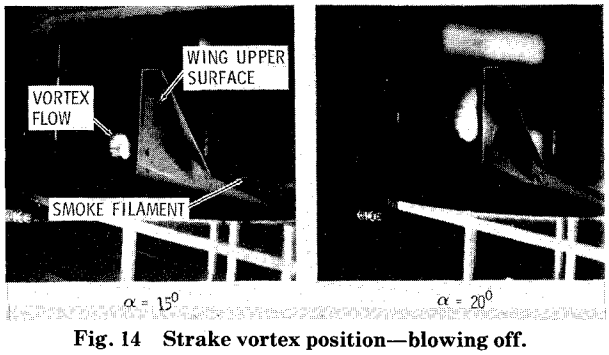

Fig. 14 Strake vortex position—blowing off.

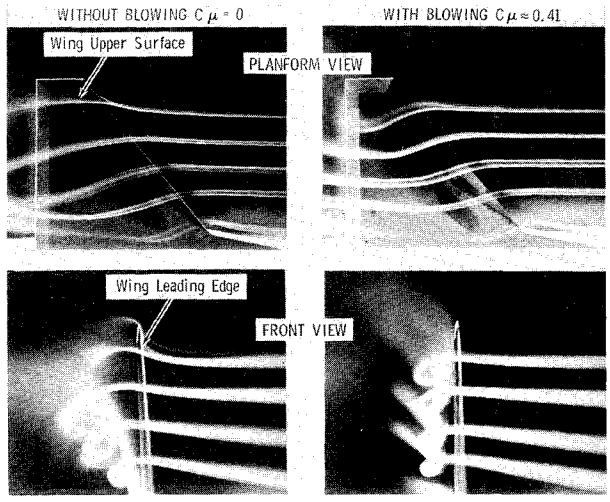

Fig. 15 Wing-strake planform streamlines, $\alpha = 20°$.

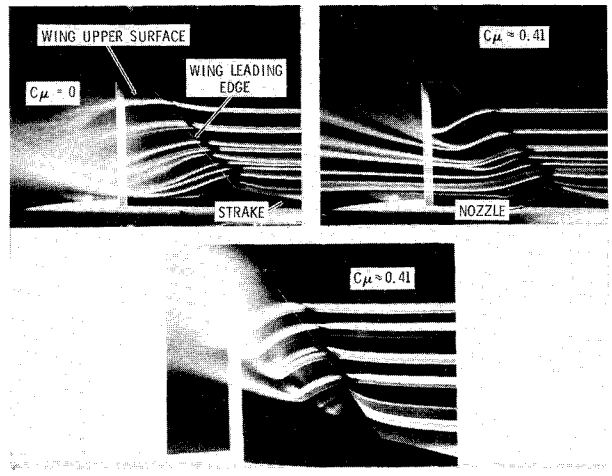

Fig. 16 Wing-strake planform streamlines, $\alpha = 25°$.

the outer panel is stalled. The vortex, enhanced by blowing, is seen to lie along the wing leading edge. The lower photograph shows a vortex core direction about parallel to the leading edge. The inboard streamlines are noted in the right-hand picture to curve over the leading-edge vortex and flow smoothly over the aft wing surface, indicating a re-attached flow behind the leading-edge vortex. The uniform streamline pattern downstream of the wing is evidence that an improved flowfield in the tail vicinity can result from the enhanced vortex flow. Thus blowing is expected to have a favorable impact on directional stability at high angles of attack.

Strake Blowing. Force and moment data are summarized in Fig. 17. Strake blowing is seen to intensify the strong vortex shed from the strake at the highest angles of attack but has little effect on the low-alpha performance.

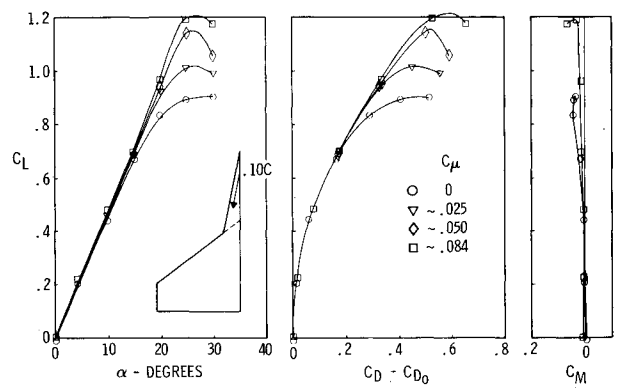

Fig. 17 Wing-strake force data—strake blowing.

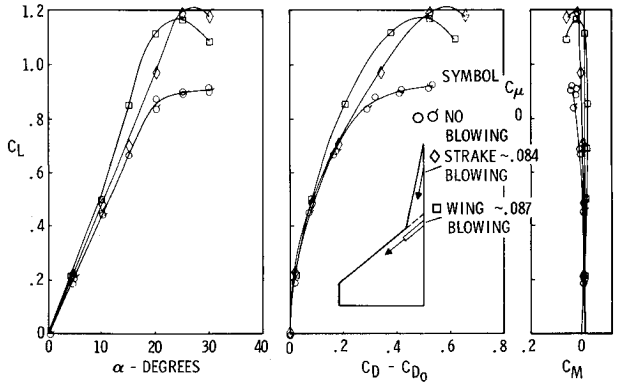

Fig. 18 Comparison of wing and strake blowing.

The natural vortex is strong for the highly swept strake; thus breakdown does not occur at as low an angle of attack as would be expected for a lower sweep. Blowing is then effective only at high angle of attack. The 0.10C nozzle location shown was found to be clearly superior to a 0.20c position which was also tested.

It is of interest to compare the relative merits of strake blowing and wing-panel blowing. Fig. 18 presents such a comparison at a blowing rate of $C_\mu \sim 0.085$. The wing blowing is noted to be effective at lower angles of attack, whereas the strake blowing is most effective at higher angles of attack. These trends are expected, since vortex breakdown occurs at lower angles of attack for wings with low-leading-edge sweep. As evidenced in the flow visualization studies, blowing tends to be effective in delaying vortex burst by intensifying and aiding in formation of the vortex system. The experimental setup did not permit simultaneous blowing of the strake and the wing.

Conclusions

The study has demonstrated that blowing directed along the general core direction of the leading-edge vortex can significantly increase the vortex lift for sharp-leading-edge planforms. Comparisons with the Polhamus suction-analogy theory for the 60° delta wing indicates that moderate blowing delays the vortex breakdown phenomena to higher angles of attack. As a result significant improvements in lift and drag-polar are possible where vortex breakdown is occurring over the wing.

It is suggested that gains in lift beyond the full suction-analogy value may be possible for high blowing rates. These gains can accrue in the form of an effective increased aspect ratio when the vortex is forced outboard from the wing tip by blowing.

For low wing sweep, the blowing appears to aid in the development of the leading-edge vortex system, thus providing improved aerodynamic performance for the wing. The payoff for blowing is greater for wings with low sweep than for wings with high sweep, where the natural vortex is strong without augmentation.

The suction-analogy theory provides a useful tool for estimating the potential benefits of vortex augmentation for a given planform. Further, the theory may form the basis of a semiempirical method for predicting the blowing effectiveness and the resulting lift and drag for thin wings.

References

[1]Ringleb, F. O., "Separation Control by Trapped Vortices," *Boundary Layer and Flow Control,* Vol. 1, 1961, edited by G. V. Lachmann, Pergamon Press, New York, 1961, pp. 265–294.

[2]Cornish, J. J., III, "High Lift Applications of Spanwise Blowing," ICAS Paper 70-09, Sept. 1970, Rome, Italy.

[3]Dixon, C. J., "Lift and Control Augmentation by Spanwise Blowing over Trailing-Edge Flaps and Control Surfaces," AIAA Paper 72-781, Los Angeles, Calif., 1972.

[4]Werle, H., "On Vortex Bursting," Note Technique 175, 1971, Office National d'Etudes et de Recherches, Chatillon, France.

[5]Wentz, W. H., Jr. and Kohlman, D. L., "Wind Tunnel Investigations of Vortex Breakdown on Slender Sharp-Edged Wings," CR 98737, Nov. 1968, NASA.

[6]Polhamus, E. C., "Predictions of Vortex-Lift Characteristics by a Leading-Edge Suction Analogy," *Journal of Aircraft,* Vol. 8, No. 4, April 1971, pp. 193–199.